RESEARCH ARTICLE | JANUARY 03 2024

Radiation effects of high-fluence reactor neutron on Ni/β-Ga_2O_3 Schottky barrier diodes FREE

Special Collection: (Ultra)Wide-bandgap Semiconductors for Extreme Environment Electronics

Leidang Zhou ; Hao Chen ; Tongling Xu; Jinlu Ruan; Yuru Lai ; Yuxin Deng ; Jiaxiang Chen ; Xinbo Zou ; Xing Lu ; Liang Chen ; Xiaoping Ouyang

Appl. Phys. Lett. 124, 013506 (2024)
https://doi.org/10.1063/5.0185271

Applied Physics Letters ARTICLE pubs.aip.org/aip/apl

Radiation effects of high-fluence reactor neutron on Ni/β-Ga_2O_3 Schottky barrier diodes

Cite as: Appl. Phys. Lett. **124**, 013506 (2024); doi: 10.1063/5.0185271
Submitted: 30 October 2023 · Accepted: 19 December 2023 ·
Published Online: 3 January 2024

Leidang Zhou,[1,2] Hao Chen,[1] Tongling Xu,[3] Jinlu Ruan,[4] Yuru Lai,[3] Yuxin Deng,[3] Jiaxiang Chen,[5] Xinbo Zou,[5] Xing Lu,[3,a)] Liang Chen,[4,a)] and Xiaoping Ouyang[4]

AFFILIATIONS

[1]School of Microelectronics, Xi'an Jiaotong University, Xi'an 710049, People's Republic of China
[2]State Key Laboratory of Multiphase Flow in Power Engineering, Xi'an Jiaotong University, Xi'an 710049, China
[3]State Key Laboratory of Optoelectronic Materials and Technologies, School of Electronics and Information Technology, Sun Yat-sen University, Guangzhou 510275, People's Republic of China
[4]Radiation Detection Research Center, Northwest Institute of Nuclear Technology, Xi'an 710024, People's Republic of China
[5]School of Information Science and Technology, Shanghai Tech University, Shanghai 201210, China

Note: This paper is part of the APL Special Collection on (Ultra)Wide-bandgap Semiconductors for Extreme Environment Electronics.
[a)]**Authors to whom correspondence should be addressed:** lux86@mail.sysu.edu.cn and Chenl_nint@163.com

ABSTRACT

This study investigates the broad-energy-spectrum reactor-neutron irradiation effects on the electrical characteristics of Ni/β-Ga_2O_3 Schottky barrier diodes (SBDs), where the irradiated neutron fluence was up to $1 \times 10^{16}\,cm^{-2}$. On the one hand, the high neutron fluence of $10^{16}\,cm^{-2}$ resulted in a reduction in forward current density by two orders of magnitude and an extremely high on-resistance property due to the radiation-generated considerable series resistance in the SBD. On the other hand, the irradiation brought little influence on the Ni/β-Ga_2O_3 Schottky contact, since the extracted ideality factor and barrier height from temperature-dependent current–voltage (I–V–T) characteristics showed no significant changes after the radiation. Moreover, the capacitance–voltage (C–V) characterization revealed that the net carrier density in the β-Ga_2O_3 material was only reduced by 25% at the neutron fluence of $10^{15}\,cm^{-2}$ but a significant reduction by 2–3 orders at $10^{16}\,cm^{-2}$. Within the neutron fluence range of $2 \times 10^{14}\,cm^{-2}$ up to $10^{16}\,cm^{-2}$, the carrier removal rates trended to be saturated with the increased fluences, following an exponential regular. In addition, the C–V measurement on the $10^{16}\,cm^{-2}$ irradiated sample exhibited an obvious frequency dispersion, and the extracted carrier distribution was not uniform.

Electronic devices operating in space require excellent radiation tolerance and temperature characteristics due to temperature variability and high-energy particle irradiation.[1–3] Gallium oxide (Ga_2O_3) possesses outstanding physical properties, such as a wide bandgap (4.5–4.9 eV) and a high breakdown electric field ($8\,MV\cdot cm^{-1}$), making it a promising candidate for high-power devices, radiation detectors, and several other applications.[4–8] Although the large bandgap and the high displacement energies of Ga and O atoms theoretically allow extending Ga_2O_3-based devices' operation to high temperatures and high radiation environments, the actual radiation tolerance and the failure mechanism of the devices at high radiation environments still require to be explored further. Neutrons are the most penetrating particles among various types of space radiation particles, and even cosmic neutron radiation can affect electronic devices on the Earth. Therefore, studying the tolerance of Ga_2O_3-based devices to neutron irradiation is essential for their aerospace and nuclear applications.[2,9–11] Previous research has investigated the neutron irradiation of Ga_2O_3-based devices below the neutron fluence of $10^{15}\,cm^{-2}$ before destroying the devices and mainly focused on the quantitative change in the performances. Although a few reports have studied the defects generation mechanism and the effect of carrier removal of the β-Ga_2O_3 material at a high neutron fluence of $10^{17}\,cm^{-2}$, the relationship between the material parameters and device performances still needs to be established.[1,12–17] Thus, to evaluate the limitation of radiation resistance of the Ga_2O_3 devices, it is of interest to explore the study of the neutron irradiation effects on the Ga_2O_3 devices to a higher neutron fluence and reveal the critical factors of the degradation of the devices' characteristics faced in such an environment.

This study experimentally investigated the influence of reactor-neutron irradiation on the performance of β-Ga_2O_3 Schottky barrier diodes (SBDs), where the highest irradiation fluence reached $10^{16}\,cm^{-2}$. The irradiation source is provided by the Xi'an Pulsed Reactor (XAPR), with neutron energies ranging from 0 to 20 MeV. The paper analyzed the electrical characteristics of β-Ga_2O_3 SBDs irradiated by three fluence levels and focused on the changes at the fluence of $10^{16}\,cm^{-2}$ based on I–V–T and C–V measurements.

Figure 1(a) presents a schematic diagram of the β-Ga_2O_3 SBD fabricated in this study. Vertical SBDs were fabricated using a (010) UID β-Ga_2O_3 substrate grown by the edge-defined film-fed growth (EFG) method with an effective carrier density of 1×10^{17}–$2\times10^{17}\,cm^{-3}$. The substrate was about 1 mm thick and $10\times15\,mm^2$ in size and was treated by a double-side chemical mechanical polishing (CMP) process. Initially, the substrate was cleaned with acetone and isopropanol, followed by a four-cycle de-ionized (DI) water rinse and N_2 blow drying. After that, a Ti/Al/Ni/Au (15 nm/80 nm/20 nm/60 nm) metal stack was electron beam evaporated on the backside of the substrate, followed by a 40-s rapid annealing at 700 °C in a N_2 ambient to form an Ohmic contact between Ti and β-Ga_2O_3. Subsequently, a circular Schottky anode electrode with a radius of 300 μm was created on the front side of the substrate through standard photolithography, electron beam evaporation of Ni/Au (20 nm/60 nm) metal layers, and liftoff. Finally, four pieces of samples were cut from the substrate, and three of them were used for the reactor-neutron radiation with the fluence of 2×10^{14}, 10^{15}, and $10^{16}\,cm^{-2}$, respectively, in Xi'an pulsed reactor (XAPR). The electric characteristics of each sample were measured using Keysight 1500 and a Lakeshore probe station with a temperature range from 75 to 325 K.

Figure 1(b) shows the current–voltage (I–V) characteristics of SBDs with and without reactor-neutron irradiation at room temperature (300 K). The forward current density remained nearly unchanged at the fluences of 2×10^{14} and $10^{15}\,cm^{-2}$. However, when the fluence reached $10^{16}\,cm^{-2}$, a significant reduction in the forward current density was observed, decreasing by approximately two orders of magnitude compared to the pre-irradiation state. Moreover, the reverse current density decreased as fluence increased, with a maximum reduction of roughly four orders of magnitude at the fluence of $10^{16}\,cm^{-2}$. To further investigate the influence of the reactor-neutron irradiation on the SBDs characteristics of the Ni/β-Ga_2O_3 SBDs, the critical parameters such as ideality factor (η) and Schottky barrier height (Φ_B) were derived from the thermionic emission equation,[12] and the special on-resistance ($R_{on,sp}$) was defined by (dV/dJ),

$$J = A^*T^2\exp\left(-\frac{q\phi_B}{kT}\right)\left[\exp\left(\frac{qV}{\eta kT}\right)-1\right], \tag{1}$$

where A is the area of the SBDs, T is temperature, k is Boltzmann constant, and q is elementary charge. A^* stands for the Richardson constant of $33.7\,A\cdot(cm\,K)^{-2}$.[18]

Specifically, the extracted η and Φ_B for the irradiated samples at fluences of 2×10^{14}, 10^{15}, and $10^{16}\,cm^{-2}$ were 1.21, 1.07, 1.00 and 1.07, 1.12, 1.17 V, respectively, showing comparable values to the pristine sample of 1.08 and 1.15 V. In contrast, the trend of $R_{on,sp}$ at different neutron influences dramatically increased when the fluence reached $10^{16}\,cm^{-2}$. As shown in Fig. 1(c), the forward $R_{on,sp}$ exhibited a slight increase from 29 to 33 mΩ cm^2 below the neutron fluence of $10^{16}\,cm^{-2}$. However, at the fluence of $10^{16}\,cm^{-2}$, the $R_{on,sp}$ rapidly increased to around 12 000 mΩ cm^2, which was responsible for the simultaneous deduction of both forward current and reverse current of the SBDs. These results indicated that reactor-neutron irradiation had a suppressive effect on the current of the Ni/β-Ga_2O_3 SBD associated with resistance of the β-Ga_2O_3 material and the Ohmic contact, and especially significant impact occurred within the neutron fluence range from 10^{15} to $10^{16}\,cm^{-2}$.

The temperature-dependent I–V characteristics were measured further to study the neutron-irradiated effects on the SBDs. Figures 2(a)–2(d) depict the forward I–V–T characteristics of the pristine sample and irradiated samples at different neutron fluences and Figs. 2(e)–2(h) show the extracted $R_{on,sp}$ of each sample. When the neutron fluences were below $10^{16}\,cm^{-2}$, the forward current density of the devices increased monotonically with the rising temperatures from 75 to 325 K, and the extracted $R_{on,sp}$ were concentrated within the range of 20–40 mΩ cm^2. However, for the higher irradiated (fluence of $10^{16}\,cm^{-2}$) sample, the I–V curves below 200 K were hardly measured, and the $R_{on,sp}$ experienced a regular deduction against the temperature. This phenomenon was explained by the high series resistance at a fluence of $10^{16}\,cm^{-2}$, rather than the Schottky contact, which dominated the $R_{on,sp}$ of the SBDs.[19]

Moreover, Figs. 2(i) and 2(j) illustrate the extracted values of the η and Φ_B for all the devices according to the thermionic emission model. It can be observed that the η decreased monotonically with the temperatures, while the Φ_B increased monotonically. This temperature-dependent behavior aligns with the non-uniformity of the barrier height at the Schottky interface.[20–22] The thermionic emission model assumes the presence of non-uniform regions at the

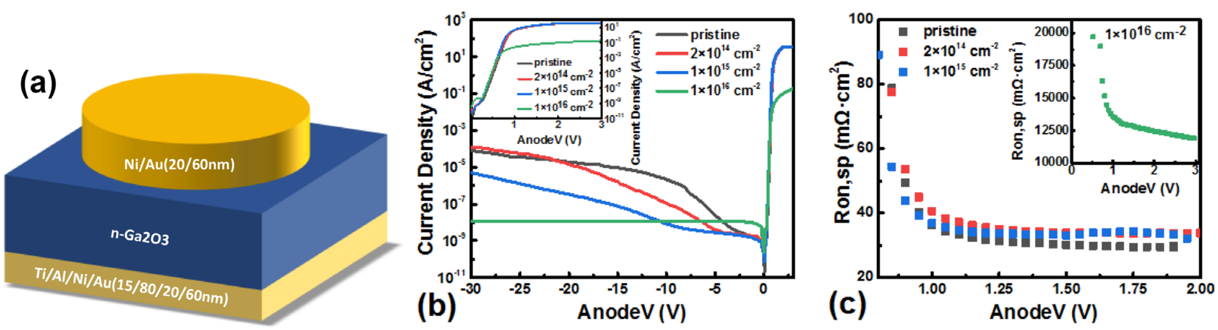

FIG. 1. (a) Schematic of the irradiated Ni/β-Ga_2O_3 Schottky barrier diodes (SBDs). (b) Typical I–V characteristics of the pristine sample and irradiated samples at neutron fluences of 2×10^{14}, 10^{15}, and $10^{16}\,cm^{-2}$ at 300 K; inset shows the forward I–V characteristics. (c) Typical $R_{on,sp}$ of the samples at 300 K; inset shows the results under neutron fluence of $10^{16}\,cm^{-2}$.

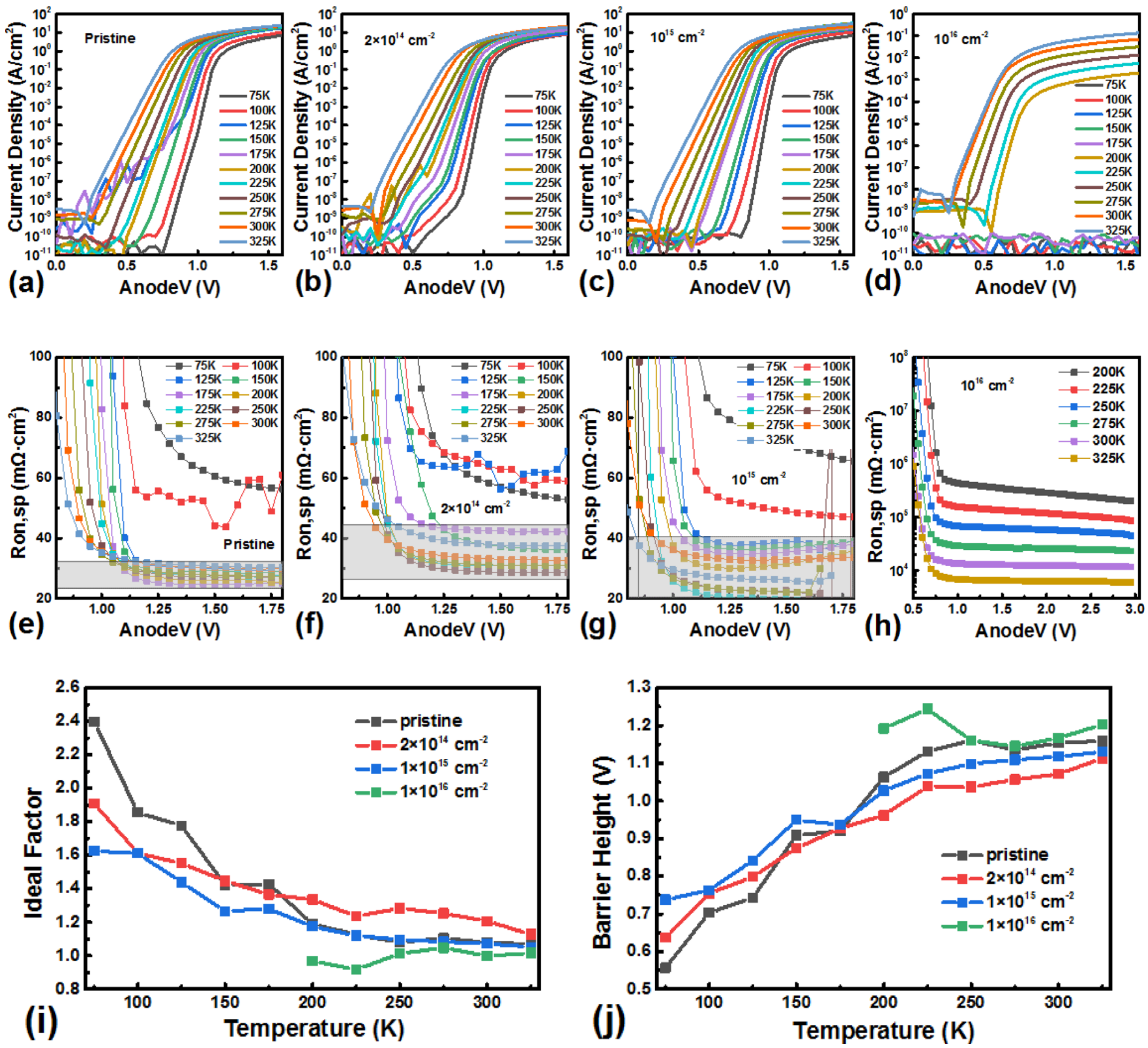

FIG. 2. (a)–(d) *I–V–T* characteristics and (e)–(h) on-resistance property of the irradiated Ni/β-Ga_2O_3 SBDs for the pristine sample and irradiated samples at neutron fluences of, 2×10^{14}, 10^{15}, and 10^{16} cm^{-2}; temperature-dependence, (i) ideality factor, and (j) barrier height curves of the irradiated SBDs.

metal–semiconductor interface, manifesting as patches with different barrier heights on the nanoscale.[20] At lower temperatures, carrier conduction is dominated by those flowing through regions with relatively low barrier heights. Conversely, at higher temperatures, carrier conduction is dominated by those flowing through regions with relatively higher barrier heights.[23] This temperature-dependent anomalous behavior of η and Φ_B can be described by the following model:

$$\phi = \bar{\phi}_0 - \frac{q\sigma^2}{2kT}, \tag{2}$$

$$\frac{1}{\eta} - 1 = -\rho_2 + \frac{q\rho_3}{2kT}. \tag{3}$$

In this model, σ represents the zero-bias standard deviation of the SBH distribution, which quantifies the degree of non-uniformity at the metal–semiconductor interface. $\bar{\phi}_0$ is the average zero-bias barrier height. ρ_2 and ρ_3 are the voltage-related coefficients for SBH and σ, respectively.

According to Figs. 2(c) and 2(d), the non-uniformity of the Schottky barrier height has no significant changes after irradiation. Notably, despite remarkable changes in the *I*–*V* characteristics of the devices occurring at a fluence of 10^{16} cm^{-2}, the value of the ideality factor remained very close to 1, which is still suitable for the thermionic emission model. This indicates that the Ni/β-Ga_2O_3 Schottky contact maintained well radiation tolerance even under high-fluence neutron irradiation.

To verify the origin of the high resistance of the samples under the reactor-neutron irradiation, the *C*–*V* characteristics analysis of the Ni/β-Ga_2O_3 SBDs was performed at 300 K with a frequency of 100 kHz on both irradiated and non-irradiated devices shown in Fig. 3(a). A reduction in capacitance after neutron irradiation was observed, and especially at the fluence of $10^{16}\,\mathrm{cm}^{-3}$, the capacitance of the SBD degraded two to three orders of magnitude more than others. The net carrier density (N_D–N_A) in the β-Ga_2O_3 can be extracted from the $1/C^2$ curves in Fig. 3(b) using the following formula:

$$N_D - N_A = -\frac{2}{q\varepsilon\varepsilon_0 A^2}\cdot\frac{1}{\frac{dC^{-2}}{dV}}, \tag{4}$$

where A is the area of the SBD, ε is the relative dielectric constant, ε_0 is the vacuum dielectric constant, N_D is the donor density, and N_A is the acceptor density.

Figure 3(c) shows the detailed carrier distribution along the depth in the UID β-Ga_2O_3. The uniform net carrier density of the pristine sample and irradiated samples at fluences of 2×10^{14} and $10^{15}\,\mathrm{cm}^{-2}$ were 1.833×10^{17}, 1.524×10^{17}, and $1.334\times10^{17}\,\mathrm{cm}^{-3}$, respectively. The drop in the net carrier density unveiled the reason for the capacitance reduction earlier. Associated with the degradation of forward current density in irradiated devices, the removal of net carrier density derived from the neutron irradiation on Ni/β-Ga_2O_3 SBD contributed to the increasing resistance, for the neutron irradiation could generate deep-level defects in the semiconductor and capture free carriers.[14] The inset of Fig. 3(c) displays a much lower net carrier density with an average value of around $5\times10^{14}\,\mathrm{cm}^{-3}$ at a fluence of $10^{16}\,\mathrm{cm}^{-2}$, about two to three orders of the pre-irradiation level decreased due to the high density of deep-level traps caused by neutron irradiation. To qualify the reduction of the net carrier density under different neutron fluences, the carrier removal rates[1] of the irradiated SBDs were calculated to be 154.5, 49.9, and $18.28\,\mathrm{cm}^{-1}$ for the fluences of 2×10^{14}, 10^{15}, and $10^{16}\,\mathrm{cm}^{-2}$. Notably, the carrier removal rates of the irradiated SBDs exhibited a decreasing trend and might have already reached a relatively limiting point at the neutron fluence of $10^{16}\,\mathrm{cm}^{-2}$. Thus, it can be postulated that the carrier removal quantity may adhere to an exponential model before the device is not severely damaged by irradiation, because the reduction of net carrier density cannot be beyond the initial value of the material. Figure 3(d) shows the fitted curve of the carrier removal quantity using an exponential model,

$$y = y_0\left[1-\exp\left(-\frac{x}{t_0}\right)\right], \tag{5}$$

where x is the neutron fluence, y is the reduction of net carrier density corresponding to the neutron fluence of x, y_0 is the initial net carrier density of the material, t_0 is a coefficient related to the material property, and the slope of the curve (dy/dx) is the carrier removal rate.

According to the fitting curve in Fig. 3(d), the y_0 was extracted to be $(1.849\pm0.263)\times10^{17}\,\mathrm{cm}^{-3}$, which was consistent with the net carrier density ($1.833\times10^{17}\,\mathrm{cm}^{-3}$) of the pristine sample. This nonlinear carrier removal rate has rarely been reported, because the nonlinearity property will occur at a much high neutron fluence. More in-depth investigations are needed to understand the fundamental physics of the nonlinear neutron radiation effect on the Ga_2O_3 material and devices, which will provide more instruments for designing the devices in aerospace and radiation applications.

To determine the non-uniform carrier distribution of the $10^{16}\,\mathrm{cm}^{-2}$ irradiated sample shown in the inset of Fig. 3(c), the frequency-dependent C–V characteristics were measured at 1, 10, 100, and 500 kHz. Figure 4(d) showed an obvious frequency dispersion at a low frequency of $10^{16}\,\mathrm{cm}^{-2}$ sample, which was not found in other samples [Figs. 4(a)–4(c)]. Figure 4(e) presents the carrier distribution with depth at different frequencies, showing the increased net carrier density with the frequency below 100 kHz and un-uniform distributions at each frequency. The abnormal C–V results at the high neutron fluence of $10^{16}\,\mathrm{cm}^{-2}$ were attributed to the high density of radiation-generated deep-level traps in the β-Ga_2O_3 material.[12] In general, many deep-level traps were generated and captured the free electron causing

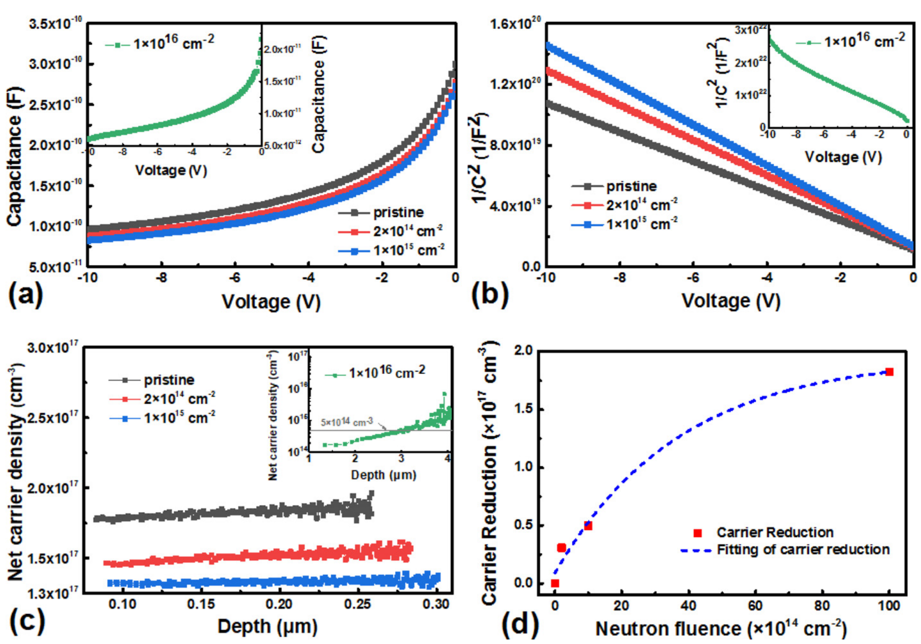

FIG. 3. (a) C–V characteristics in 100 kHz. (b) $1/C^2$ in 100 kHz. (c) Distribution of the net carrier density (N_D–N_A) of pristine sample and irradiated samples at neutron fluences of 2×10^{14}, 10^{15} at 300 K; all the insets show the results under neutron fluence of $10^{16}\,\mathrm{cm}^{-2}$. (d) Carrier reduction against the neutron fluences.

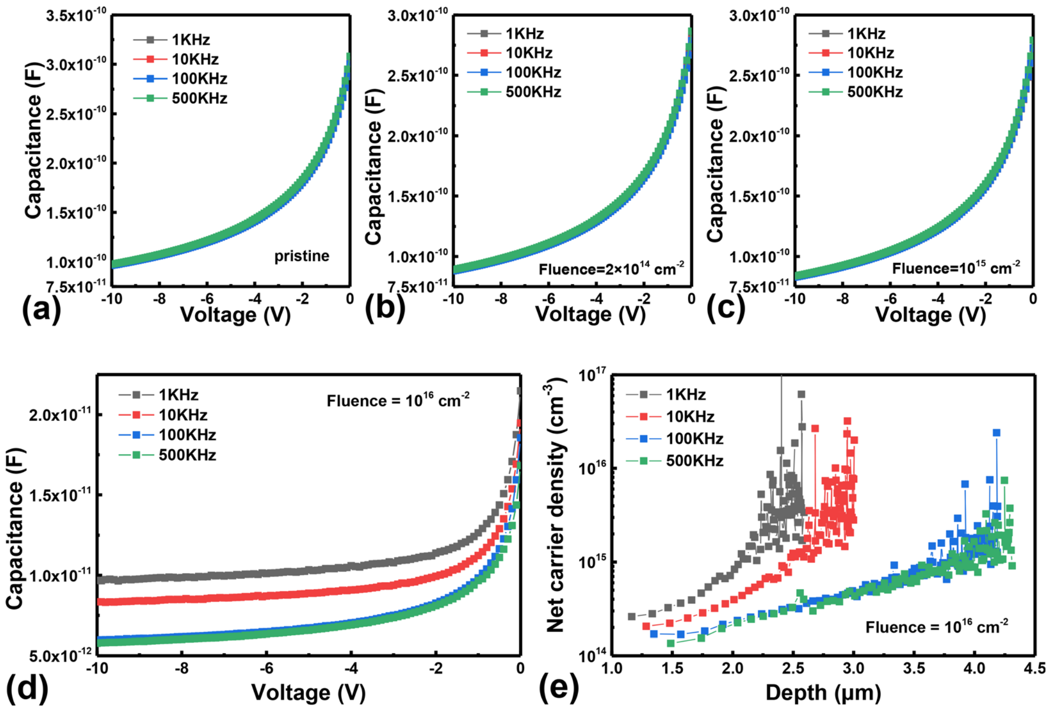

FIG. 4. (a)–(c) C–V frequency curves of the samples of pristine, neutron fluence of $2 \times 10^{14}\,\mathrm{cm}^{-2}$, and $10^{15}\,\mathrm{cm}^{-2}$. (d) C–V characteristics against neutron fluence of $10^{16}\,\mathrm{cm}^{-2}$ at different frequencies. (e) Net carrier density (N_D–N_A) distribution against the frequency under neutron fluence of $10^{16}\,\mathrm{cm}^{-2}$.

the reduction in the net carrier density. Then the occupied deep-level traps had a long time constant to release and capture the electron,[24] and the captured electrons were excited under a high applied electric field. Thus, the C–V-measured net carrier density increased with the bias voltage (or the depth of depletion region) and decreased with applied frequency.

In summary, the effects of reactor-neutron irradiation with different fluences on the electrical performances of the Ni/β-Ga_2O_3 SBDs have been studied in this work. At low neutron fluences of 2×10^{14} and $10^{15}\,\mathrm{cm}^{-2}$, the I–V and C–V characteristics of the SBDs were slightly influenced by the fluence of the reactor neutron. However, at the neutron fluence of $10^{16}\,\mathrm{cm}^{-2}$, both the forward current density and the reverse current density decreased rapidly due to the extremely high resistance caused by the net carrier density reduction. In addition, the Schottky barrier inhomogeneity of the SBDs showed no significant change under the reactor-neutron irradiation up to the fluence range of $10^{16}\,\mathrm{cm}^{-2}$. According to the C–V measurement, the net carrier density for the pristine and irradiated devices at low fluences showed a uniform distribution but a non-uniform distribution at the high neutron fluence of $10^{16}\,\mathrm{cm}^{-2}$. These phenomena and the frequency dispersion of the SBDs indicated that the high density of the deep-level traps was generated at high neutron fluence of $10^{16}\,\mathrm{cm}^{-2}$, and a significant impact occurred during the neutron fluence from 10^{15} to $10^{16}\,\mathrm{cm}^{-2}$. In addition, the carrier removal rates under the neutron irradiation were discovered to be well-fitted in the exponential model but not a constant in the β-Ga_2O_3.

This work was supported by the National Natural Science Foundation of China under Grant No. 62204198, the Guangdong Basic and Applied Basic Research Foundation under Grant No. 2022A1515012163, and the Fundamental Research Funds for the Central Universities under Grant No. 22120220626.

AUTHOR DECLARATIONS

Conflict of Interest

The authors have no conflicts to disclose.

Author Contributions

Leidang Zhou: Conceptualization (equal); Data curation (equal); Formal analysis (equal); Funding acquisition (equal); Investigation (lead); Validation (equal); Writing – original draft (equal). **Hao Chen:** Data curation (equal); Formal analysis (equal); Investigation (equal); Writing – original draft (equal). **Tongling Xu:** Data curation (equal). **Jinlu Ruan:** Methodology (equal); Project administration (equal); Resources (equal). **Yuru Lai:** Formal analysis (equal). **Yuxin Deng:** Formal analysis (equal). **Jiaxiang Chen:** Data curation (equal). **Xinbo Zou:** Data curation (equal); Resources (equal). **Xing Lu:** Conceptualization (equal); Data curation (equal); Formal analysis (equal); Funding acquisition (equal); Writing – original draft (equal). **Liang Chen:** Conceptualization (equal); Data curation (equal); Formal analysis (equal); Funding acquisition (equal); Investigation (equal); Methodology (equal); Project administration (lead); Resources (lead); Writing – original draft (equal). **Xiaoping Ouyang:** Conceptualization (equal); Investigation (equal); Methodology (equal); Project administration (lead); Resources (equal); Supervision (lead).

DATA AVAILABILITY

The data that support the findings of this study are available within the article.

REFERENCES

[1] J. Kim, S. J. Pearton, C. Fares, J. Yang, F. Ren, S. Kim, and A. Y. Polyakov, "Radiation damage effects in Ga_2O_3 materials and devices," J. Mater. Chem. C **7**, 10 (2019).

[2] C. P. Irvine, A. Stopic, M. T. Westerhausen, M. R. Phillips, and C. Ton-That, "Enhancement of excitonic and defect-related luminescence in neutron transmutation doped β-Ga_2O_3," Phys. Rev. Mater. **6**(11), 114603 (2022).

[3] X. Xia, J.-S. Li, R. Sharma, F. Ren, M. Abu Jafar Rase, S. Stepanoff, N. Al-Mamun, A. Haque, D. E. Wolfe, S. Modak, L. Chernyak, M. E. Law, A. Khachatrian, and S. J. Pearton, "Radiation damage in the ultra-wide bandgap semiconductor Ga_2O_3," ECS J. Solid State Sci. Technol. **11**, 095001 (2022).

[4] X. Lu, L. Zhou, L. Chen, X. Ouyang, B. Liu, J. Xu, and H. Tang, "Schottky x-ray detectors based on a bulk β-Ga_2O_3 substrate," Appl. Phys. Lett. **112**, 103502 (2018).

[5] L. Zhou, H. Chen, Y. Deng, S. Zhang, L. Chen, X. Lu, and X. Ouyang, "Alpha particle detection based on a NiO/β-Ga_2O_3 heterojunction diode," Appl. Phys. Lett. **123**, 161103 (2023).

[6] X. Ji, C. Lu, Z. Yan, L. Shan, X. Yan, J. Wang, J. Yue, X. Qi, Z. Liu, W. Tang, and P. Li, "A review of gallium oxide-based power Schottky barrier diodes," J. Phys. D: Appl. Phys. **55**(44), 443002 (2022).

[7] C. Lu, X. Ji, Z. Liu, X. Yan, N. Lu, P. Li, and W. Tang, "A review of metal–semiconductor contacts for β-Ga_2O_3," J. Phys. D: Appl. Phys. **55**(46), 463002 (2022).

[8] A. Grillo, J. Barrat, Z. Galazka, M. Passacantando, F. Giubileo, L. Iemmo, G. Luongo, F. Urban, C. Dubourdieu, and A. Di Bartolomeo, "High field-emission current density from β-Ga_2O_3 nanopillars," Appl. Phys. Lett. **114**, 193101 (2019).

[9] B. R. Tuttle, N. J. Karom, A. O'Hara, R. D. Schrimpf, and S. T. Pantelides, "Atomic-displacement threshold energies and defect generation in irradiated β-Ga_2O_3: A first-principles investigation," J. Appl. Phys. **133**(1), 015703 (2023).

[10] L. N. Cojocaru, "Defect-annealing in neutron-damaged β-Ga_2O_3," Radiat. Eff. **21**(3), 157–160 (2006).

[11] B. E. Kananen, L. E. Halliburton, K. T. Stevens, G. K. Foundos, and N. C. Giles, "Gallium vacancies in β-Ga_2O_3 crystals," Appl. Phys. Lett. **110**(20), 202104 (2017).

[12] J. Lee, A. C. Silverman, E. Flitsiyan, M. Xian, F. Ren, and S. J. Pearton, "Impact of neutron irradiation on electronic carrier transport properties in Ga_2O_3 and comparison with proton irradiation effects," Radiat. Eff. Defects Solids **178**(5–6), 680–698 (2023).

[13] E. Farzana, A. Mauze, J. B. Varley, T. E. Blue, J. S. Speck, A. R. Arehart, and S. A. Ringel, "Influence of neutron irradiation on deep levels in Ge-doped (010) β-Ga_2O_3 layers grown by plasma-assisted molecular beam epitaxy," APL Mater. **7**(12), 121102 (2019).

[14] J. Liu, Z. Han, L. Ren, X. Yang, G. Xu, W. Hao, X. Zhao, S. Yang, D. Lu, Y. Han, X. Hou, and S. Long, "Oxygen vacancies and local amorphization introduced by high fluence neutron irradiation in β-Ga_2O_3 power diodes," Appl. Phys. Lett. **123**(11), 112106 (2023).

[15] S. Yue, X. Zheng, Y. Hong, X. Zhang, F. Zhang, Y. Wang, X. Ma, and Y. Hao, "Effects of neutron irradiation on electrical performance of β-Ga_2O_3 Schottky barrier diodes," IEEE Trans. Electron Devices **70**(6), 3026–3030 (2023).

[16] A. Y. Polyakov, N. B. Smirnov, I. V. Shchemerov, A. A. Vasilev, E. B. Yakimov, A. V. Chernykh, A. I. Kochkova, P. B. Lagov, Y. S. Pavlov, O. F. Kukharchuk, A. A. Suvorov, N. S. Garanin, I.-H. Lee, M. Xian, F. Ren, and S. J. Pearton, "Pulsed fast reactor neutron irradiation effects in Si-doped n-type β-Ga_2O_3," J. Phys. D: Appl. Phys. **53**(27), 274001 (2020).

[17] F. Mirkhosravi, A. Rashidi, A. T. Elshafiey, J. Gallagher, Z. Abedi, K. Ahn, A. Lintereur, E. K. Mace, M. A. Scarpulla, and D. Feezell, "Effects of fast and thermal neutron irradiation on Ga-polar and N-polar GaN diodes," J. Appl. Phys. **133**(1), 015704 (2023).

[18] L. Zhou, X. Lu, L. Chen, X. Ouyang, B. Liu, J. Xu, and H. Tang, "Leakage current by Poole–Frenkel emission in Pt Schottky contacts on $(\bar{2}01)$ β-Ga_2O_3 grown by edge-defined film-fed growth," ECS J. Solid State Sci. Technol. **8**(7), Q3054–Q3057 (2019).

[19] S. E. Swirhun and R. M. Swanson, "Temperature dependence of specific contact resistivity," IEEE Electron Device Lett. **7**(3), 155–157 (1986).

[20] P. P. Sundaram, F. Liu, F. Alema, A. Osinsky, B. Jalan, and S. J. Koester, "Characterization of (001) β-Ga_2O_3 Schottky diodes with drift layer grown by MOCVD," Appl. Phys. Lett. **122**(23), 232105 (2023).

[21] P. R. S. Reddy, V. Janardhanam, K.-H. Shim, V. R. Reddy, S.-N. Lee, S.-J. Park, and C.-J. Choi, "Temperature-dependent Schottky barrier parameters of Ni/Au on n-type (001) β-Ga_2O_3 Schottky barrier diode," Vacuum **171**, 109012 (2020).

[22] A. Jadhav, L. A. M. Lyle, Z. Xu, K. K. Das, L. M. Porter, and B. Sarkar, "Temperature dependence of barrier height inhomogeneity in β-Ga_2O_3 Schottky barrier diodes," J. Vac. Sci. Technol. B **39**(4), 040601 (2021).

[23] A. Di Bartolomeo, F. Giubileo, G. Luongo, L. Iemmo, N. Martucciello, G. Niu, M. Fraschke, O. Skibitzki, T. Schroeder, and G. Lupina, "Tunable Schottky barrier and high responsivity in graphene/Si-nanotip optoelectronic device," 2D Mater. **4**, 015024 (2016).

[24] G. I. Roberts and C. R. Crowell, "Capacitive effects of Au and Cu impurity levels in Pt-N type Si Schottky barriers," Solid-State Electron. **16**(1), 29–38 (1973).